# Near-Infrared Tunable Filters for Cryogenic Wide Field Imagers

S. Satyapal, M. A. Greenhouse, R. Barclay, D. Amato, R. Barry, C. Holt, S. Irish, J. Kuhn, A. Kutyrev, A. Morrel – NASA Goddard Space Flight Center
B. Arritt – Air Force
T. Hilgeman, L. Lesyna, N. Fonneland, Northrop Grumman Corporation

NEXT GENERATION
NGST
SPACE TELESCOPE

## Overview

Fabry-Perot (FP) interferometers enable wide field imaging spectroscopy of galactic or extragalactic sources over a wide field of view. Low resolution imaging spectroscopy is required for astronomical surveys of high redshift galaxies or imaging spectroscopy of broad emission line features in galactic or nearby extragalactic sources (see figure below). Unlike other options for variable interference filters (circular variable filters, linear variable filters, etc.) Fabry-Perots do not require the often difficult optical constraint of producing a small pupil in the optical system. In such systems, FPs ease the size requirements on flight instrument filter inventory and can be combined with gratings and grisms to enable both spatial and spectral multiplexing in a single instrument package. We anticipate near-term applications for cryogenic tunable filters for the Next Generation Space Telescope (NGST), the Stratospheric Observatory for Infrared Astronomy (SOFIA), and 8 m ground-based telescopes. We plan for this work to be made available to NGST and other instrument builders as a GSFC work package.

Near-infrared tunable bandpass filters are being designed for the baseline wide field camera of the NGST Integrated Science Instrument Module (ISIM) . This Demonstration Unit for Low Order Cryogenic Etalon (DULCE), is designed to demonstrate a high efficiency scanning Fabry-Perot etalon operating in interference orders 1-4 at 30 K with a high stability DSP based servo control system. DULCE has heritage in a Northrop Grumman system designed for 1st order operation at 300 K, and is being developed jointly by GSFC and NGC as an option to satisfy NGST requirements. In this application, scanning etalons will illuminate the focal plane arrays with a single order of interference to enable wide field low resolution (50 < R < 200) hyperspectral imaging over a wide range of galaxy redshifts.

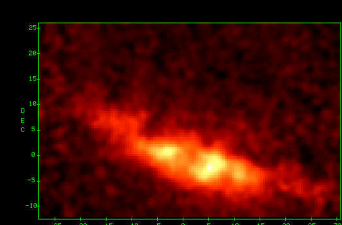


**3.3 μm Dust Feature Image of the Starburst Galaxy M82.**

Dulce will enable low resolution imaging spectroscopy over a wide field of view of nearby extragalactic and galactic sources.

## DULCE Highlights

- Variable spectral resolution in single cryogenic etalon ( 50 < R < 200) enabled through high precision long stroke cryogenic actuators
- Low order cryogenic operation enabled by mechanical assembly for sub micron etalon gap at temperature of 30 K
- Low phase dispersion multilayer dielectric coatings for 0.6-5.3 μm allow etalon tuning characteristics that are constant in wavelength in low order operation
- Etalon plate flatness of λ/100 at 632 nm permits reflectance finesse-limited operation
- High stability low drift DSP-based servo control system controls cavity spacing to < 5 nm
- Compact design
- Only available cryogenic Fabry-Perot for low order operation in the near-IR

## Integrated Science Instrument Module Camera

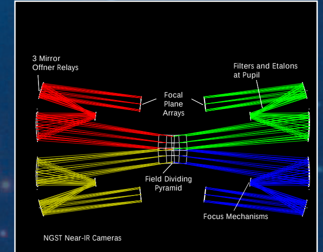


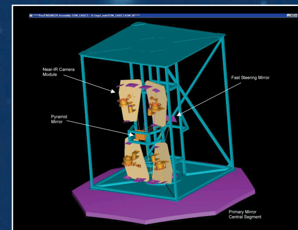


The ISIM near-infrared wide field camera employs a pyramid beam divider to apportion a 16 square arc-min field of view over four identical camera channels. One channel is shown here in detail. Each channel utilizes a 4096 x 4096 focal plane array covering 4 square arc-min. The baseline ISIM also includes a near-infrared multi-object spectrometer and mid-infrared imaging spectrograph not show here.

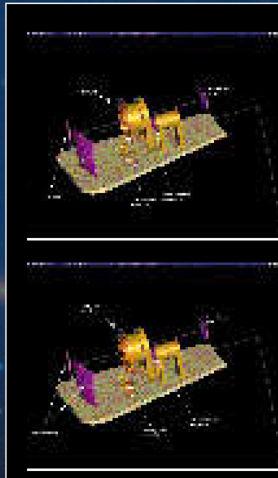

Each camera channel includes a focusing Offner relay, filter wheel, and retractable tunable filter.

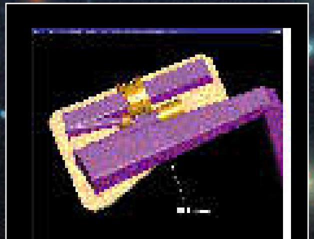

The opto-mechanical layout provides sufficient pupil access to accommodate the tunable filter etalon assembly. The etalon shown is 80 mm OD x 40 mm long x 40 mm clear aperture.

## Mechanical Design

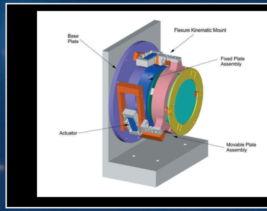


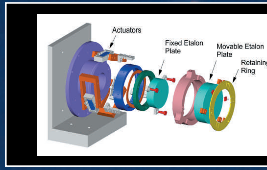


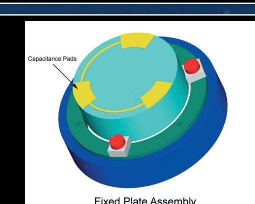


Capacitance pads are etched onto the etalon plates to measure directly the Fabry-Perot gap spacing.

**Mechanical gain compensates for PZT strain loss at cryogenic temperatures.**

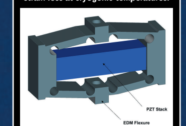


Current Actuators: Magnified expansion low voltage PZT actuator selected for DULCE yields 20 μm of strain at 30 K. Prototype tested at 30K

**Cryogenic Actuator Testbed**

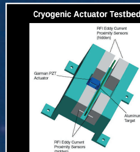


This setup is designed to characterize the cryogenic properties of the actuators. The contraction upon cooling and the cryogenic strain is measured using eddy current sensors.

**Future Actuators**

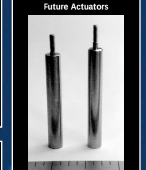

COTS super conducting magnetostrictive actuators produced by Energen Inc. will be used in a future iteration of DULCE. These actuators yield a factor of 7 increase in cryogenic strain relative to the PZT actuators we are currently using. The resulting increase in etalon scan range and therefore spectral resolution will allow a single mechanical design to satisfy an even wider range of science applications.

## Thermal Modeling

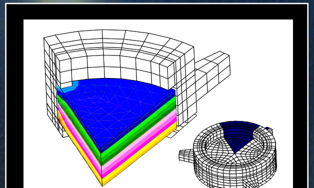

Finite element analysis is used to model thermal deformation of the etalon plates and the mechanical assembly.

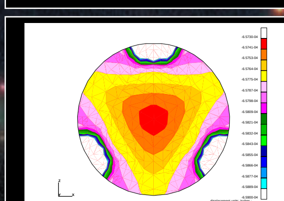

Finite element analysis is used to model thermal deformation of the etalon plates and the mechanical assembly.

## Coating Design

**Dielectric mirror coatings that control the reflection phase change to approximate an ideal metallic reflector are critically important for etalons that must operate in low orders of interference. Control of the reflection phase change allows one to achieve small effective etalon gap spacings and etalon tuning characteristics that are constant with wavelength. Northrop Grumman has developed such coatings.**

### The Effect of Coating Phase Dispersion

The etalon transmission $T_{FP}(\sigma)$ is given by

$$T_{FP}(\sigma) = \frac{T(\sigma)^2}{(1-R(\sigma)^2)}\left(1 + \frac{4R(\sigma)}{(1-R(\sigma))^2}\sin^2(2\pi\mu d\sigma\cos\theta - \phi(\sigma))\right)^{-1},$$

where T and R are the coating transmission and reflectivity, μ is the gap index of refraction, d is the physical gap length, σ is the wavenumber of the incident light, θ is the chief ray angle of incidence, φ(σ) is the phase shift upon reflection. In the case of dielectric reflections for which φ(σ) ≠ 0, the right hand term does not vanish at d = 0. In applications requiring low order (small d) operation, the effective optical thickness of the reflective coating resulting from φ(σ) must be taken into account in modeling the effective etalon gap.

Taking a first order Taylor series approximation to φ(σ) about the center of the bandpass $\sigma_0$, we can write the argument of the sin function as

$$\delta = \left(2\pi\mu d\cos\theta - \frac{d\phi}{d\sigma}\right)\sigma - \phi_0$$

where $\sigma_0$ is a constant. We define the effective optical thickness of the coating $d_{stack}$ as

$$d_{stack} = -\frac{1\pi}{2\sigma}\frac{d\phi}{d\sigma}.$$

so that $\delta = 2\pi(\mu d\cos\theta + d_{stack})\sigma - \phi_0$. Resonances occur when $\delta = n\pi$, where n is the order of interference

$$\sigma_n = \frac{n}{2(\mu d\cos\theta + d_{stack})} + \frac{\phi_0}{2\pi(\mu d\cos\theta + d_{stack})}.$$

The order sorting requirement is determined by the wavenumber spacing fsr between successive resonances

$$fsr = \frac{1}{2(d + d_{stack})}.$$

and the spectral resolution Δσ is

$$\Delta\sigma = \frac{fsr}{N_{tot}}$$

where $N_{tot}$ is the total finesse of the etalon plates. Since the phase dispersion $\frac{d\phi}{d\sigma} < 0$, **fsr is maximised when low phase dispersion coatings are used.**

### Low-Order Fabry-Perot Interferometer Equivalents

Dielectric Stack is Characterized by Reflectivity and Phase

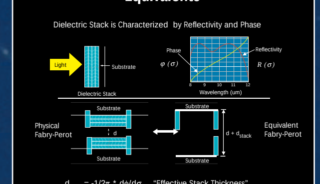


$d_{stack} = -1/2\pi * d\phi/d\sigma$ "Effective Stack Thickness"

### Effect of Phase on Free Spectral Range

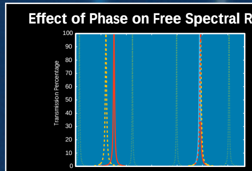


Theoretical transmission spectra for a Fabry-Perot interferometer (d=6.7μm, R=~95%).
... Conventional mirror with no phase control.
-- Mirrors with ideal phase characteristics.
- Low-Dispersion mirrors.

### Phase Measurements With Fizeau Interferometer

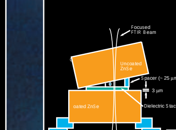


Attributes of Measurement Technique
- Asymmetric Fabry-Perot
- Single Mirror Measurement
  - ZnSe Reference Flat
- No Sophisticated Alignment
- Easy Access to Multiple Orders

### Fizeau Interferometer Relationships

Asymmetric Fabry-Perot Transmission

$$A(\sigma) = \frac{T_1T_2}{(1-\sqrt{R_1}\sqrt{R_2})}\frac{1}{1+\frac{4\sqrt{R_1}\sqrt{R_2}}{(1-\sqrt{R_1}\sqrt{R_2})^2}\sin^2\left(2\pi\mu d\sigma\cos\theta - \frac{\varphi_1(\sigma)}{2} - \frac{\varphi_2(\sigma)}{2}\right)}$$

Phase of Stack Is Determined by

$$n\pi = 2\pi\mu d\sigma\cos\theta - \frac{\varphi(\sigma)_{FP}}{2} - \frac{\pi}{2}$$

ZnSe phase is π

For Normal Incidence & Air Gap

$$\varphi(\sigma_n) = (2n+1)\pi - 4\pi d\sigma_n$$

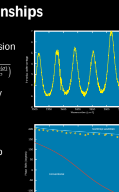

## Servo Design

### DULCE Actuator Characterization

- Low voltage (130 V) PZT
- Expect stroke ~ 20 um at 30 K.
- Cryogenic stroke and frequency response measured with laser ranging Zygo interferometer.
- Three actuators under evaluation:
  – Garman Systems Inc.
  – EMF Technologies Inc.
  – COTS superconducting magnetostrictive actuators

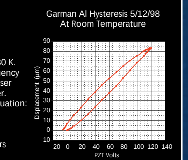


### DULCE Electro-Mechanical System Block Diagram

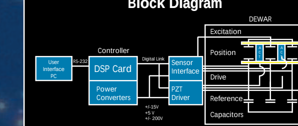


- •Capacitor Bridge reference capacitors located in etalon for stability.
- •Sensor interface located near etalon for low noise susceptibility.
- •Modular approach facilitates change to different sensors or drivers.
- •DSP enables flexibility for design modifications.

### DULCE Control Electronics

- Implemented on TMS320c40 DSP board developed at GSFC.
- Same controller to be used on HIRDLS magnetic bearing and ZEPHYR wind LIDAR.
- Capacitive sensor demodulation uses lock-in amplifier for high stability and noise rejection. Will provide options for either analog or DSP implementation.
- NGC has demonstrated 0.5 nm rms stability with earlier system.
- 16-bit A/D and D/A converters.
- Capacitor excitation generated digitally on sensor card for high precision and flexibility.

### DULCE Electronic Architecture

Controller Card:
TMS320c40 DSP, RAM, EEPROM, Actel gate-array, serial interface and parallel digital interface.

Sensor Card:
Charge amplifiers, analog lock-in demodulator, A/D converters, D/A converter and EEPROM for capacitor sine-wave excitation generation, selector switch for demodulated or raw signals, multiplexor.

Driver Card:
D/A converters, power amplifiers, multiplexor.

Power Card:
Power supplies for +/- 200V, +/-12V, and +5V.

### Control System First-Order Model

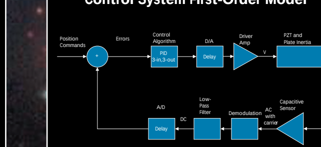


There will be coupling between each actuator and each sensor. A translation matrix will weight contributions from each respective part. The actual values above have not yet been determined. Measurements and analysis are currently on-going